Received: 10 December 2017 | Revised: 7 March 2018 | Accepted: 15 March 2018

DOI: 10.1111/cas.13583

ORIGINAL ARTICLE

WILEY Cancer Science

Downregulation of miR-491-5p promotes gastric cancer metastasis by regulating SNAIL and FGFR4

Ting Yu[1] | Li-na Wang[1] | Wei Li[2] | Qian-fei Zuo[1] | Meng-meng Li[1] | Quan-ming Zou[1] | Bin Xiao[1]

[1]National Engineering Research Center of Immunological Products, Department of Microbiology and Biochemical Pharmacy, College of Pharmacy, Third Military Medical University, Chongqing, China

[2]Department of Pharmacy, Southwest Hospital, Third Military Medical University, Chongqing, China

Correspondence
Bin Xiao and Quan-ming Zou, Department of Microbiology and Biochemical Pharmacy, College of Pharmacy, Third Military Medical University, Chongqing, China.
Emails: binxiaotmmu@163.com (B. Xiao); qmzou2007@163.com (Q.-M. Zou)

Funding information
National Natural Science Foundation of China, grant number 81202310; Chongqing Youth Science and Technology Talent Training Project, grant number cstc2014kjrc-qnrc10008.

Gastric cancer (GC) is among the most fatal cancers in China. MicroRNAs (miRNAs) are versatile regulators during GC development and progression. miR-491-5p has been demonstrated to act as a tumor suppressor in several types of cancer. However, the role of miR-491-5p in GC metastasis remains unknown. Here, we found that miR-491-5p was significantly decreased in GC tissues compared with adjacent non-cancerous tissues, and low miR-491-5p level was associated with large tumor size. Overexpression of miR-491-5p significantly suppressed GC cell epithelial-to-mesenchymal transition (EMT) and tumor metastasis in vitro and in vivo. Mechanistically, SNAIL was identified as a direct target of miR-491-5p. The silencing of SNAIL phenocopied the tumor suppressive function of miR-491-5p, whereas re-expression of SNAIL in GC cells rescued the EMT markers and cell migratory ability that were inhibited by miR-491-5p. In addition, miR-491-5p inhibited FGFR4 indirectly. Inhibition of FGFR4 also decreased the SNAIL level and impaired EMT and cell migration. Taken together, these findings indicate that downregulation of miR-491-5p promoted GC metastasis by inducing EMT via regulation of SNAIL and FGFR4.

KEYWORDS
FGFR4, gastric cancer, metastasis, miR-491-5p, SNAIL

1 | INTRODUCTION

Gastric cancer (GC) is a commonly diagnosed cancer and is among the most fatal cancers in China. The incidence and mortality of GC in China in 2015 were estimated to be 679 100 cases and 498 000 cases, respectively.[1] Due to early diagnoses and the development of therapeutic methods, the incidence and mortality of GC have slowly decreased in the past decade among both Chinese males and females. However, the outcomes of GC patients, especially those with metastatic disease, remain very poor.[1] Thus, further exploration of the precise molecular mechanisms that occur during GC development and progression is urgently needed.

MicroRNAs (miRNAs) have been demonstrated to act as oncogenes or tumor suppressors in several types of cancer. In GC, miRNAs are differentially expressed, and unique miRNAs are associated with different histological subtypes and the progression and prognosis of the disease.[2] miR-491-5p has been identified as a tumor suppressor in several types of cancer and acts to regulate cell proliferation, apoptosis, migration, invasion and chemoresistance.[3-5] However, the role of miR-491-5p in GC is largely unclear. Sun et al[6] found that miR-491-5p is downregulated in GC tissues, and the restoration of miR-491-5p led to retarded tumor growth through the targeting of Wnt3a/beta-catenin signaling. However, the comprehensive function of miR-491-5p in GC, especially GC with metastatic statuses, remains unknown.

Metastasis is the most significant process in the progression of GC. In China, more than 80% of GC patients are diagnosed at an advanced stage that is often accompanied by metastatic disease,

which contributes to the low 5-year survival rate.[1,7] The epithelial–mesenchymal transition (EMT) is a critical step in the initiation of GC migration and invasion. E-cadherin is a hallmark of epithelial integrity and a major component of adherens junctions. Mutations and methylations of E-cadherin frequently occur in GC.[7] SNAIL is known to be a transcriptional repressor of E-cadherin. Overexpression of SNAIL inhibits the transcription of E-cadherin, induces EMT and favors tumor metastasis. Our previous findings also demonstrated that SNAIL acts as a promoter of GC growth and metastasis.[8] Fibroblast growth factor receptor (FGFR4) is a tyrosine kinase and cell surface receptor for fibroblast growth factor 19 (FGF19). The FGF19-FGFR4 axis causes a loss of β-catenin-E-cadherin binding, which indicates that this axis could possibly potentiate tumor metastasis.[9] In GC, FGFR4 is reported to be highly expressed in cancerous tissues and to be associated with cancer progression. Overexpression of FGFR4 affects GC cell proliferation and apoptosis.[10] Here, we further elaborate the functions of SNAIL and FGFR4, and how these genes are regulated in GC.

In the present study, we investigate the roles of miR-491-5p in GC development and progression, particularly in GC metastasis. We identified SNAIL as a direct target of miR-491-5p, and FGFR4 was inhibited indirectly by miR-491-5p. miR-491-5p-mediated inhibition of these 2 genes resulted in the suppression of EMT and GC metastasis.

2 | MATERIAL AND METHODS

2.1 | Clinical samples

Forty pairs of frozen gastric cancer tissues and matched nonmalignant tissues were obtained from the Southwest Hospital of the Third Military Medical University (Chongqing, China). None of these patients had received chemotherapy or radiotherapy before surgery. Patients with infectious diseases, autoimmune diseases or multiple-primary cancers were excluded from the study. All samples were collected with the consent of the patients, and the experiments were approved by the Ethics Review Board of the Third Military Medical University.

2.2 | Cell culture

The GC cell lines SGC-7901, BGC-823, AGS and HGC-27 and the normal epithelial cell line GES were obtained from the Cell Bank of the Chinese Academy of Sciences (Shanghai, China). HEK293T cells were obtained from HanBio (Shanghai, China). The cell lines were cultured individually with RPMI 1640 (SGC-7901, AGS, HGC-27 and GES) or DMEM (BGC-823 and HEK293T) supplemented with 10% FCS at 37°C with 5% CO_2.

2.3 | RNA isolation and quantitative real-time PCR

Total RNA was extracted using the Trizol (Invitrogen, Carlsbad, CA, USA) method. The expression of miRNA was measured using a TaqMan MicroRNA Reverse Transcription Kit and TaqMan MicroRNA Assays (Applied Biosystems, Foster City, CA, USA). The data were normalized to the endogenous U6 snRNA. For mRNA detection, reverse transcription was performed using PrimeScript RT Master Mix (TaKaRa, Dalian, China). Real-time PCR was performed using SYBR (Toyobo, Japan). The data were normalized to GAPDH. The primer sequences are listed in Table S1. All quantitative real-time PCR (qRT-PCR) reactions were performed in triplicate using a Bio-Rad CFX96 real-time PCR system. The results were calculated according to the $2^{-\Delta\Delta CT}$ method.

2.4 | Transient transfection and construction of stable cell lines

MicroRNA mimics and FGFR4 siRNAs were purchased from Ribobio (Guangzhou, China). SNAIL siRNAs were obtained from Sigma-Aldrich (St Louis, MO, USA). The siRNA information is presented in Table S1. The pCMV-SNAIL and pCMV-NC vectors were purchased from OriGene (Rockville, MD, USA). All transfections in this study were performed using Lipofectamine 2000 (Invitrogen, Carlsbad, CA, USA) according to the manufacturer's instructions. The miR-491-5p-overexpression retrovirus was produced as described previously.[11] To construct the stable cell lines, cells were infected with a retrovirus encoding an miR-491-5p transcript and GFP or GFP alone (mock). Forty-eight hours later, puromycin was added to the medium (1 μg/mL). After 3 passages, the fluorescence of the cells was observed with a microscope, and the transfection efficiency was detected by qRT-PCR. The cells were then ready for use.

2.5 | Cell migration assay

Cell migration ability was measured using Transwell chambers (5-μm pore size, Costar, Cambridge, MA, USA). Briefly, cells were suspended in serum-free medium and seeded onto the upper chamber (1×10^5 cells per chamber). In the lower chamber, 300 μL of medium with 10% FCS was added as a chemoattractant. Twenty-four hours later, the cells in the upper chamber were wiped away. The cells located on the lower surface of the chamber were fixed with 4% paraformaldehyde and then stained with 0.1% crystal violet. Then, the cells in 5 randomly selected fields were photographed under a microscope (×100). The crystal violet adhering to the cells was re-dissolved with 30% acetic acid, and the absorbance values were detected at 570 nm using a microtiter plate reader (Molecular Devices).

2.6 | Cell proliferation assay

Cells were seeded at a density of 1×10^4 per well in 96-well plates and then transfected with miRNA mimics or oligonucleotides. The cell viability values were measured using Cell Counting Kit 8 (CCK8; Dojindo Laboratories, Kumamoto, Japan) at the indicated times. The absorbance values were detected at 450 nm using a microtiter plate reader (Molecular Devices).

2.7 | Cell apoptosis assay

Cells were transfected with miRNA mimics for 24 hours and then starved for 48 hours. Next, the cells were double-stained with Annexin V/7AAD (Biolegend), and the proportion of apoptotic cells was assessed by flow cytometry. The results were analyzed using FlowJo software, version 6.2.

2.8 | Animal experiments

Female BALB/c nude mice (6-8 weeks old) were purchased from the Beijing HFK Bioscience (Beijing, China). The animal experiments were performed as described previously.[12] Briefly, SGC-7901 cells that stably overexpressed miR-491-5p or the mock cells were suspended in PBS. For subcutaneous xenograft inoculation, 1×10^6 cells were injected subcutaneously into the dorsal areas of the mice (4 mice per group). Thirty days later, the mice were killed, and the tumor volumes were measured (volume = length $\times$ width^2/2). For the peritoneal dissemination assay, 1×10^6 cells were injected into the abdominal cavities of the mice (5 mice per group). Six weeks later, the mice were killed and the macroscopic nodules in the abdominal cavity were counted. For the distal pulmonary metastasis assay, 2×10^6 cells were injected into the tail vein of each mouse (5 mice per group). The mice were killed 3 months later, and the metastatic nodules in the lungs were counted. The animal studies were approved by the Institutional Animal Care and Use Committee of the Third Military Medical University.

2.9 | Luciferase assays

The wild-type and mutant 3′-UTR of human *SNAIL* and *FGFR4* were inserted into dual luciferase miRNA expression reporter vectors (pMIR-REPORT System, Applied Biosystems, CA, USA). The mutant vectors were constructed by replacing the miR-491-5p binding sites in the 3′-UTR of *SNAIL* and *FGFR4*. HEK293T cells were seeded onto 96-well plates (1×10^4 cells per well) and co-transfected with the wild-type or mutant vector (200 ng per well), the pRL-TK Renilla luciferase reporter (10 ng per well), miR-491-5p mimics or mimic NC (50 nmol/L). Twenty-four hours later, the luciferase activities were measured using the Dual Luciferase Reporter Assay (Promega, Madison, MI, USA) on a GLOMAX 20/20 luminometer (Promega). The firefly luciferase activity was normalized to Renilla luciferase activity. All assays were repeated independently 3 times and in quadruplicate.

2.10 | Western blotting

Western blotting was performed as described previously.[11] Primary antibodies against Wnt/β-Catenin Activated Targets Antibody Sampler Kit, ERK1/2, p-ERK1/2 (Thr202/Tyr204), AKT, p-AKT (Ser473), p-AKT (Thr308) (Cell Signaling Technology), SNAIL, FGFR4, Vimentin, Fibronectin and N/E-cadherin (Abcam) were used under recommended dilution. GAPDH was used as an internal reference. The signals were detected using the SuperSignal West Dura Extended Duration Substrate Kit (Thermo Scientific Pierce, Rockford, IL, USA). The results were analyzed using the Image Lab software.

2.11 | Immunohistochemistry

The xenografts were removed from the tumor-bearing mice, paraformaldehyde-fixed, paraffin-embedded and cut into 5-μm sections. For immunohistochemistry (IHC) staining, deparaffinization, endogenous peroxidase blocking and antigen retrieval were performed sequentially on the sections.[13] Then, the sections were incubated with anti-SNAIL antibody (1:100; Abcam) and stained with HRP-conjugated IgG antibody followed by diaminobenzidine. Next, the sections were counterstained with hematoxylin and examined using a microscope (Nikon Eclipse 80i, Nikon). Finally, a single pathologist, blinded to treatment groups, scored SNAIL immunostaining by assessing the percentage of SNAIL$^+$ cells multiplied by the intensity of SNAIL staining (1-3) in both the cytoplasm and nucleus of the cells.[14]

2.12 | Statistical analysis

A 2-tailed Student's *t*-test was performed to analyze the differences between the 2 groups. The relationships between 2 genes were analyzed with correlation coefficients and linear regression analyses. All data were analyzed using the GraphPad Prism software version 5.0 (GraphPad Software, La Jolla, CA, USA) and are expressed as the mean $\pm$ SD. $P \leq .05$ was considered to be statistically significant.

3 | RESULTS

3.1 | miR-491-5p is downregulated in gastric cancer tissues, and restoration of miR-491-5p suppresses cell migration and proliferation in vitro

We first analyzed the levels of miR-491-5p in 40 pairs of GC tissues and matched non-cancerous tissues via qRT-PCR. The results revealed that the expression of miR-491-5p was significantly downregulated in the GC tissues by an average of 2.87-fold. Decreases in miR-491-5p were observed in 37 of 40 (92.5%) cancerous tissues (Figure 1A). Moreover, low miR-491-5p expression was found to be correlated with large tumor size, and the level of miR-491-5p was associated with different tumor histological types (Table 1). Next, we chose BGC-823 and SGC-7901 cells for further investigation because those cells exhibited relatively higher and lower expression levels for miR-491-5p (Figure 1B). We identified the roles of miR-491-5p in GC cell migration, proliferation and apoptosis. We found that overexpression of miR-491-5p significantly inhibited the migration of both SGC-7901 and BGC-823 cells (Figure 1C and Figure S1). However, inhibition of miR-491-5p had no significant effect on cell migration (Figure S2). This result may have been caused by the relatively low endogenous abundance of miR-491-5p in SGC-7901 and BGC-823 cells. In addition, overexpression of miR-491-5p

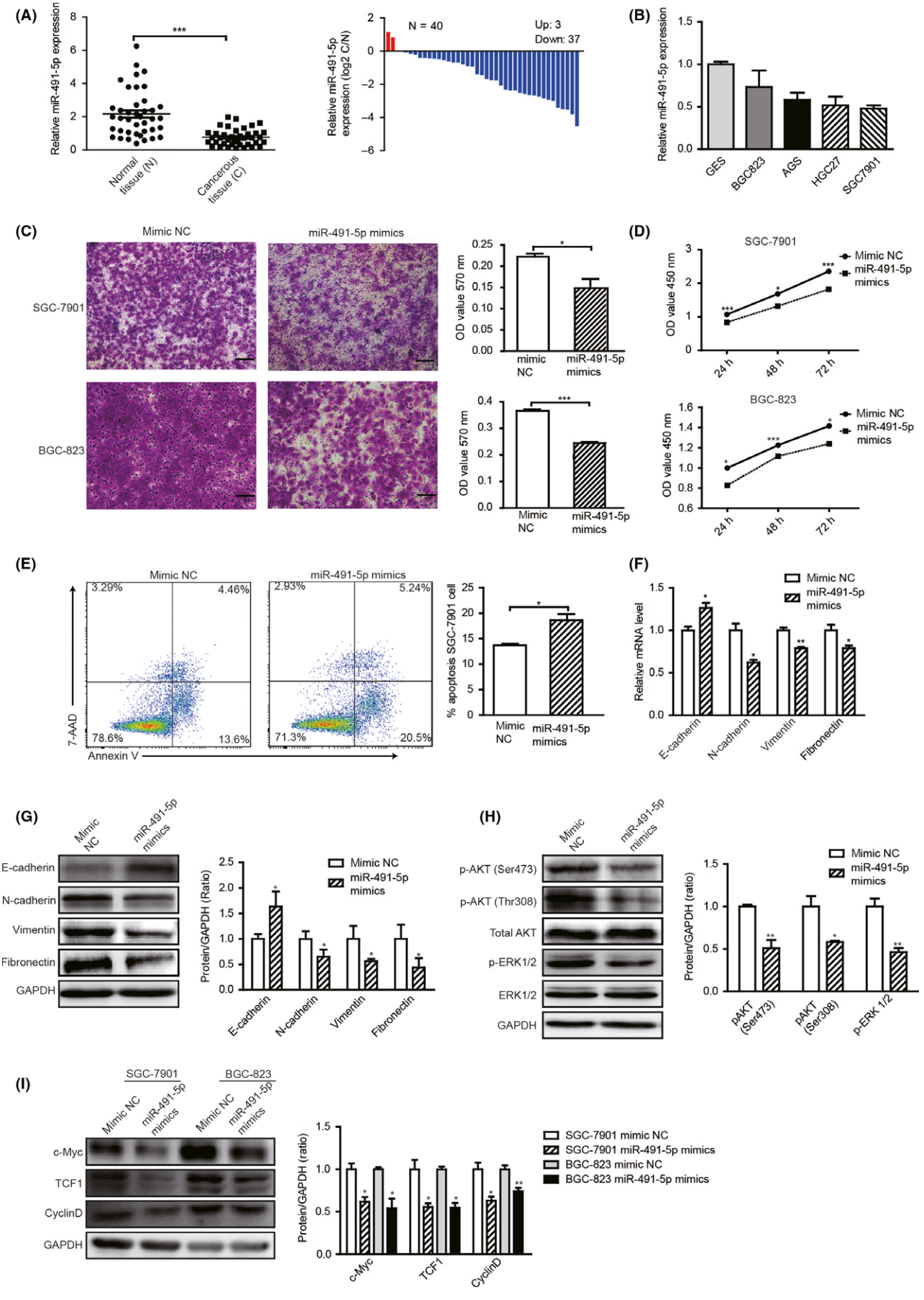
(A)
Relative miR-491-5p expression
***
Normal tissue (N)
Cancerous tissue (C)
Relative miR-491-5p expression (log2 C/N)
N = 40
Up: 3
Down: 37
(B)
Relative miR-491-5p expression
GES
BGC823
AGS
HGC27
SGC7901
(C)
Mimic NC
miR-491-5p mimics
SGC-7901
BGC-823
OD value 570 nm
mimic NC
miR-491-5p mimics
(D)
SGC-7901
BGC-823
OD value 450 nm
Mimic NC
miR-491-5p mimics
24 h
48 h
72 h
(E)
Mimic NC
miR-491-5p mimics
3.29%
4.46%
78.6%
13.6%
2.93%
5.24%
71.3%
20.5%
7-AAD
Annexin V
% apoptosis SGC-7901 cell
(F)
Relative mRNA level
E-cadherin
N-cadherin
Vimentin
Fibronectin
(G)
E-cadherin
N-cadherin
Vimentin
Fibronectin
GAPDH
Protein/GAPDH (Ratio)
(H)
p-AKT (Ser473)
p-AKT (Thr308)
Total AKT
p-ERK1/2
ERK1/2
GAPDH
Protein/GAPDH (ratio)
pAKT (Ser473)
pAKT (Ser308)
p-ERK 1/2
(I)
SGC-7901
BGC-823
c-Myc
TCF1
CyclinD
GAPDH
Protein/GAPDH (ratio)
SGC-7901 mimic NC
SGC-7901 miR-491-5p mimics
BGC-823 mimic NC
BGC-823 miR-491-5p mimics

FIGURE 1 miR-491-5p is downregulated in gastric cancer (GC) and inhibits GC cell metastasis and proliferation. A, The relative expression levels of miR-491-5p in cancerous and non-cancerous tissues (n = 40; left). The data are represented as the log2 fold changes (ΔΔCt values, C/N; right). B, The expression levels of miR-491-5p in different GC cell lines. SGC-7901 and BGC-823 cells were transfected with miR-491-5p mimics or mimic NC (50 nmol/L). C, 24 hours later, cells migration abilities were detected via Transwell assays. Scale bar = 50 μm. D, Cell viabilities were investigated using CCK8 assays at 24, 48 and 72 hours after transfection. E, 24 hours after transfection, SGC-7901 cells were starved for 48 hours, and the apoptotic cells were then detected via staining with 7-AAD and Annexin V. (F) The mRNA levels and the protein levels (G) of EMT markers, the protein levels of total AKT and ERK1/2, phosphorylated AKT and ERK1/2 (H), TCF1, c-Myc and CyclinD (I) in cells that were transfected with miR-491-5p mimics or mimic NC (50 nmol/L). G-I, representative western blots bands are presented on the left, and pooled data from n = 3 independent experiments are presented on the right. *$P < .05$, ***$P < .001$

elicited a strong inhibition of cell proliferation as early as 24 hours after transfection (Figure 1D), and promoted the apoptosis of SGC-7901 cells (Figure 1E). The above data suggest that miR-491-5p is a versatile regulator in GC cells.

Epithelial-to-mesenchymal transition is vital in the initiation of tumor metastasis. We next detected the effects of miR-491-5p on EMT molecules. The results revealed that miR-491-5p-overexpressing BGC-823 cells exhibited reduced expression of N-cadherin, vimentin and fibronectin (FN1) and increased expression of E-cadherin, which indicated that miR-491-5p inhibited EMT in BGC-823 cells (Figure 1F,G). Moreover, we found that miR-491-5p was capable of inhibiting the activation of ERK1/2 and AKT (Figure 1H), which was consistent with previous reports.[3,4,15] Overexpression of miR-491-5p also suppressed target genes of Wnt signaling, such as c-Myc, TCF-1 and CyclinD, in both the SGC-7901 and BGC-823 cells (Figure 1I). These results indicate that miR-491-5p inhibits EMT, and decreases the AKT, MAPK and Wnt signaling pathways activities in GC cells.

TABLE 1 Clinical and pathological characteristics of included patient samples

Variable	Number of patients N = 40 (%)	miR-491-5p expression mean ± SD	*P*-value
Gender			
Male	27 (68)	0.7424 ± 0.09698	.8264
Female	13 (32)	0.7795 ± 0.1365	
Age			
≥55	23 (58)	0.8088 ± 0.0865	.4509
<55	17 (42)	0.6809 ± 0.1432	
Tumor size			
<5 cm	25 (62)	0.8795 ± 0.0968	.0371*
≥5 cm	15 (38)	0.5461 ± 0.1166	
Histologic type			
Tubular adenocarcinoma	31 (78)	0.6837 ± 0.0850	.0461*
Mucinous adenocarcinoma	7 (17)	1.149 ± 0.1719	
Signet-ring cell adenocarcinoma	2 (5)	0.4682 ± 0.2705	
Histological differentiation			
Well differentiation	2 (5)	0.8123 ± 0.3448	.818
Moderate differentiation	11 (27.5)	0.6584 ± 0.1099	
Low differentiation	27 (67.5)	0.7893 ± 0.1055	
TNM stage			
I	7 (18)	0.6355 ± 0.1507	.4078
II	11 (27)	0.6382 ± 0.1118	
III	22 (55)	0.8505 ± 0.1208	
Lymph node metastasis			
Positive	27 (68)	0.8246 ± 0.1057	.1289
Negative	13 (32)	0.6088 ± 0.09005	

*$P < .05$

In addition to miR-491-5p, the miR-491 transcript produces another mature product (ie, miR-491-3p), which has been confirmed to be involved in tumor growth, metastasis and chemoresistance.[3,16] Here, we found that the expression of miR-491-3p was also significantly downregulated in GC tissues. Overexpression of miR-491-3p remarkably inhibited the migration of GC cells (Figure S3). However, considering that the expression of miR-491-3p was much lower than that of miR-491-5p in GC tissues, we chose miR-491-5p for further investigation.

3.2 | miR-491-5p targets SNAIL directly and inhibits FGFR4 indirectly in gastric cancer cells

To date, the identities of the genes regulated by miR-491-5p in GC remain unclear. Here, the candidate target genes of miR-491-5p were predicted with TargetScan, and then we performed microarray chip experiments using 5 pairs of GC tissues and their non-cancerous counterparts to identify the genes deregulated in GC.[8] Considering that the expression of miR-491-5p was decreased, we searched for intersections between the predicted target genes and the upregulated genes (759) on the microarray chips, and 37 genes were selected. We then analyzed the expression levels of the 37 candidates in the paired GC data from TCGA and found that 31 of the 37 genes were upregulated in the GC tissues. Among these genes, 15 candidates were selected because they were functionally related to cell metastasis (Figure 2A,B). We then determined whether these 15 genes were inhibited by miR-491-5p. Finally, SNAIL and FGFR4 were found to be inhibited by miR-491-5p at both the mRNA and protein levels (Figure 2C,D). We observed that the 3′-UTR of *SNAIL* contained 3 target sites for miR-491-5p, while *FGFR4* contained only 1 such site. We next constructed the luciferase reporter vectors containing the wild-type 3′-UTR sequences of *SNAIL* or *FGFR4* or the mutated binding sequences of miR-491-5p (Figure 2E). The dual

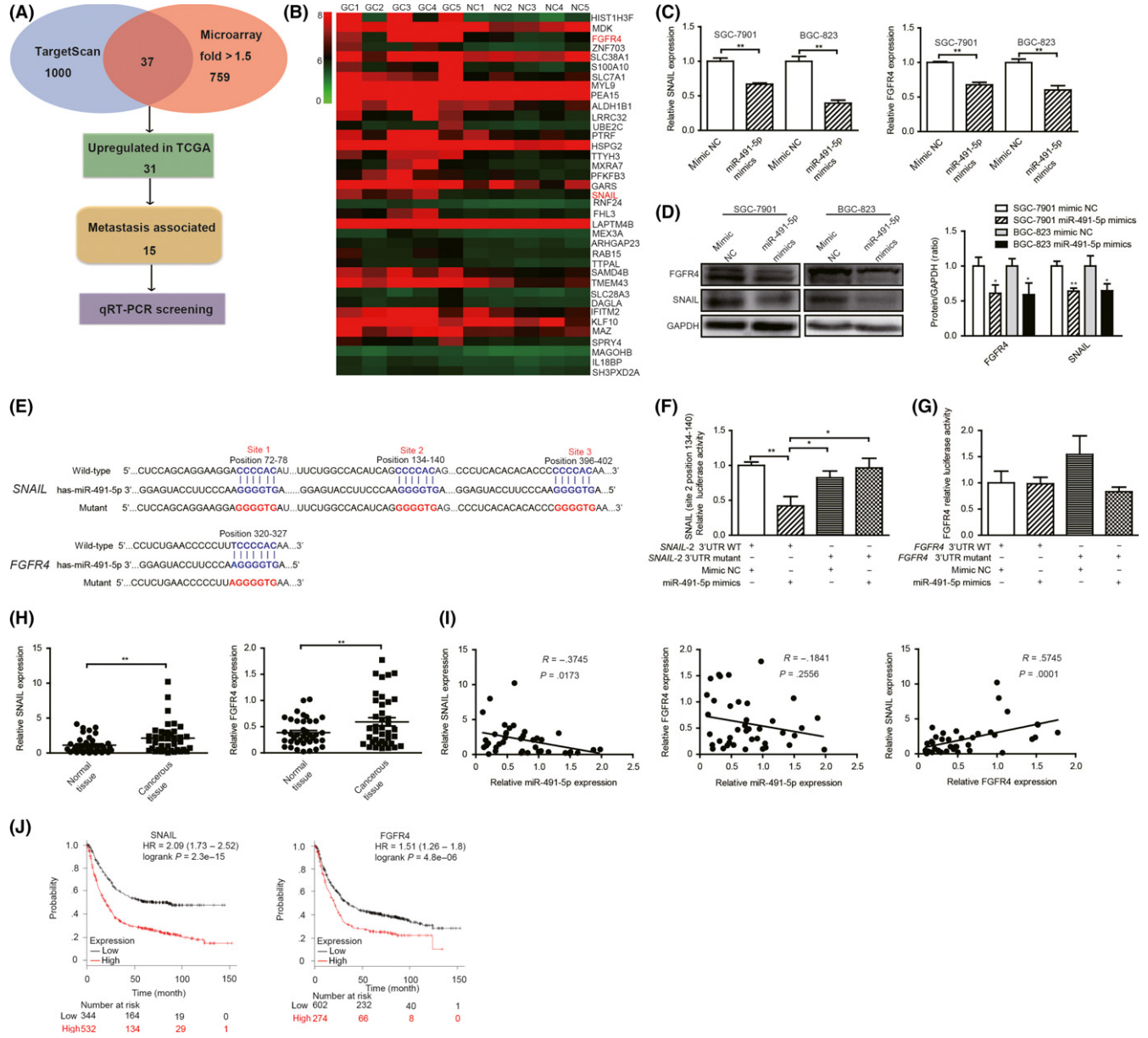

FIGURE 2 miR-491-5p inhibits SNAIL and FGFR4. A, The schematic diagram presents the process and criteria used for the selection of the candidate targets of miR-491-5p. B, The heat map shows 37 genes that were both upregulated on the microarray chips and predicted to be targeted by miR-491-5p. The mRNA levels (C) and the protein levels (D) of SNAIL and FGFR4 in cells transfected with miR-491-5p mimics or mimic NC (50 nmol/L). Left, the representative western blot bands. Right, pooled data from n = 3 independent experiments. E, The wild-type and mutated binding sequences of miR-491-5p in the 3′-UTR of *SNAIL* and *FGFR4*. F, miR-491-5p inhibits the wild-type, but not the mutant *SNAIL* (Site2, position 134-140) 3′-UTR luciferase activity. G, miR-491-5p has no effect on *FGFR4* 3′-UTR luciferase activity. H, The relative mRNA levels of SNAIL (left) and FGFR4 (right) in 40 paired gastric cancer (GC) and normal tissues. I, Correlations of SNAIL and miR-491-5p (left), FGFR4 and miR-491-5p (middle), and SNAIL and FGFR4 (right) in the 40 GC tissues. J, Kaplan-Meier plots for SNAIL and FGFR4 in the GC cohorts. The log-rank *P*-values and hazard ratios (hazard ratio: 95% confidence interval in parentheses) are presented. $^*P < .05$, $^{**}P < .01$

luciferase assay results revealed that miR-491-5p reduced the luciferase activity by 57.93% at nucleotide position 134-140 (site 2) of the *SNAIL* 3′-UTR (Figure 2F) but had no influence at the other 2 sites (Figure S4). Moreover, miR-491-5p had no effect on the luciferase activity of the FGFR4 vector (Figure 2G). These results suggest that SNAIL is a direct target of miR-491-5p, but the inhibitory effect of miR-491-5p on FGFR4 is indirect.

We next analyzed the expression levels of SNAIL and FGFR4 in 40 pairs of GC tissues and non-cancerous tissues. The results revealed that the expression levels of SNAIL and FGFR4 were significantly upregulated in the GC tissues (Figure 2H). SNAIL level was inversely correlated with miR-491-5p in the GC tissues, but there was no significant correlation between FGFR4 and miR-491-5p. Moreover, there was a positive correlation between SNAIL and

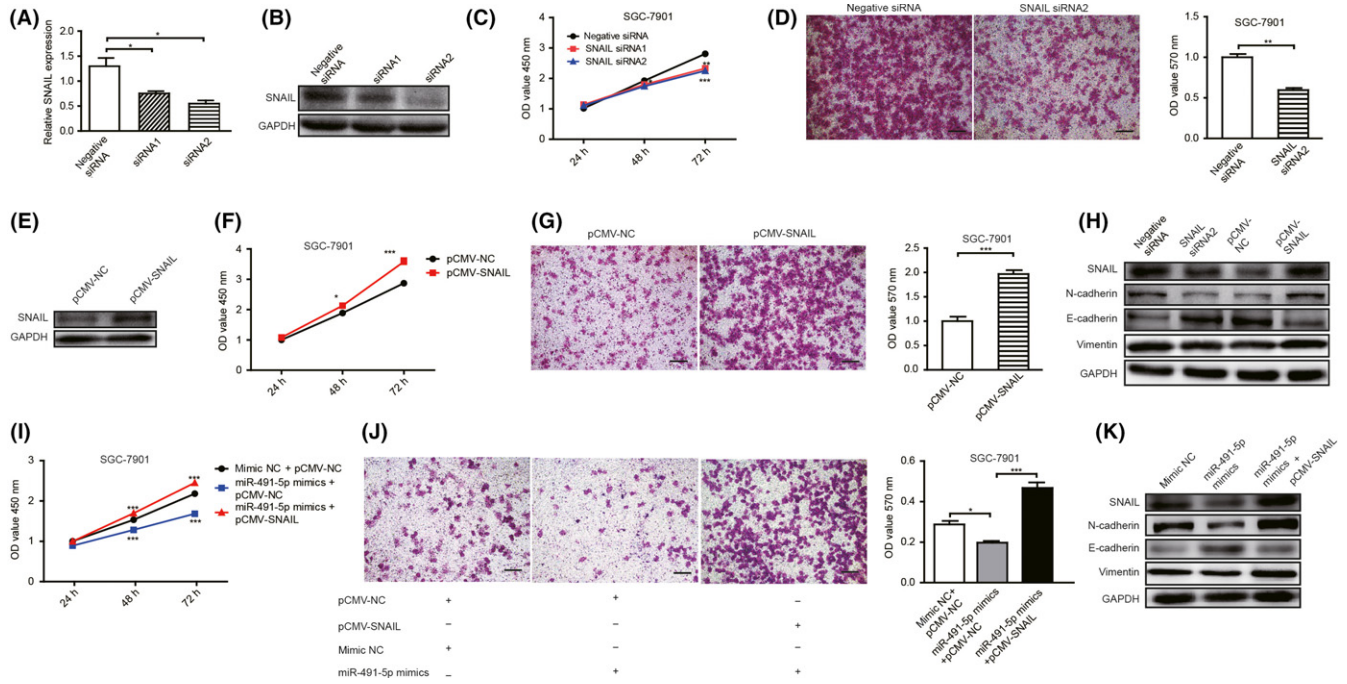

FIGURE 3 SNAIL mediates the suppressive function of miR-491-5p in gastric cancer (GC) cells. (A) The mRNA and protein (B) levels of SNAIL in cells transfected with siRNA. The proliferation (C) and migration (D) abilities of SGC-7901 cells transfected with siRNA were measured at the indicated times. E, Overexpression of SNAIL was examined via western blotting. After overexpression of SNAIL, the proliferation (F) and migration (G) abilities of SGC-7901 cells were measured at the indicated times. H, The protein levels of SNAIL, N-cadherin, E-cadherin and vimentin in SGC-7901 cells transfected with siRNA or overexpression vectors. (I) The proliferation and migration (J) abilities of SGC-7901 cells that were co-transfected with miR-491-5p mimics, pCMV-SNAIL or the individual controls were measured at the indicated times. K, The protein levels of specific genes in SGC-7901 cells that were transfected with miR-491-5p mimics alone or co-tranfected with miR-491-5p mimics and pCMV-SNAIL. Scale bar = 50 μm. $*P < .05$, $**P < .01$, $***P < .001$

FGFR4 in the GC tissues (Figure 2I). To characterize the associations of SNAIL and FGFR4 with the prognosis of GC, Kaplan–Meier survival curves were created based on the data from 876 GC patients in the KM plots database (http://kmplot.com/analysis/).[17] We found that GC patients with higher levels of SNAIL or FGFR4 had worse survival (Figure 2J). These results indicate that SNAIL and FGFR4 are dysregulated in GC and are correlated with GC prognosis.

3.3 | miR-491-5p-mediated SNAIL suppression reduces proliferation and migration of gastric cancer cells

To determine whether the inhibitory effect of miR-491-5p on GC cells is dependent on SNAIL, we first detected the function of SNAIL in GC cells. When SNAIL was inhibited using siRNA (Figure 3A,B), the proliferation and migration abilities of SGC-7901 cells were significantly decreased (Figure 3C,D), which mimicked the effect of miR-491-5p overexpression. In contrast, the restoration of SNAIL significantly promoted the proliferation and migration abilities of SGC-7901 cells (Figure 3E–G). Consistent with the effect of miR-491-5p overexpression, inhibition of SNAIL decreased the expression levels of N-cadherin and Vimentin but increased the expression of E-cadherin. Rescued expression of SNAIL had the opposite effects (Figure 3H). Furthermore, re-expression of SNAIL counteracted the effects of miR-491-5p on cell proliferation, migration and the expression of EMT molecules (Figure 3I–K). These results suggest that miR-491-5p inhibits GC cell proliferation and metastasis in a manner that depends on the regulation of SNAIL.

3.4 | FGFR4 promotes gastric cancer cell proliferation, migration and epithelial-to-mesenchymal transition

Because miR-491-5p indirectly inhibited FGFR4, we next investigated whether the inhibition of FGFR4 would affect the proliferation and metastasis of GC cells. FGFR4 was inhibited using siRNA (Figure 4A,B), and proliferation and migration assays were performed. The results revealed that inhibition of FGFR4 resulted in decreased proliferation and migration of SGC-7901 cells (Figure 4C,D). Furthermore, inhibition of FGFR4 decreased the protein levels of c-Myc and TCF1 and hall markers of EMT, including SNAIL and N-cadherin, whereas this treatment increased the E-cadherin level (Figure 4E); this pattern phenocopied the action of miR-491-5p overexpression. These results indicate that miR-491-5p-mediated indirect inhibition of FGFR4 suppresses GC growth and metastasis.

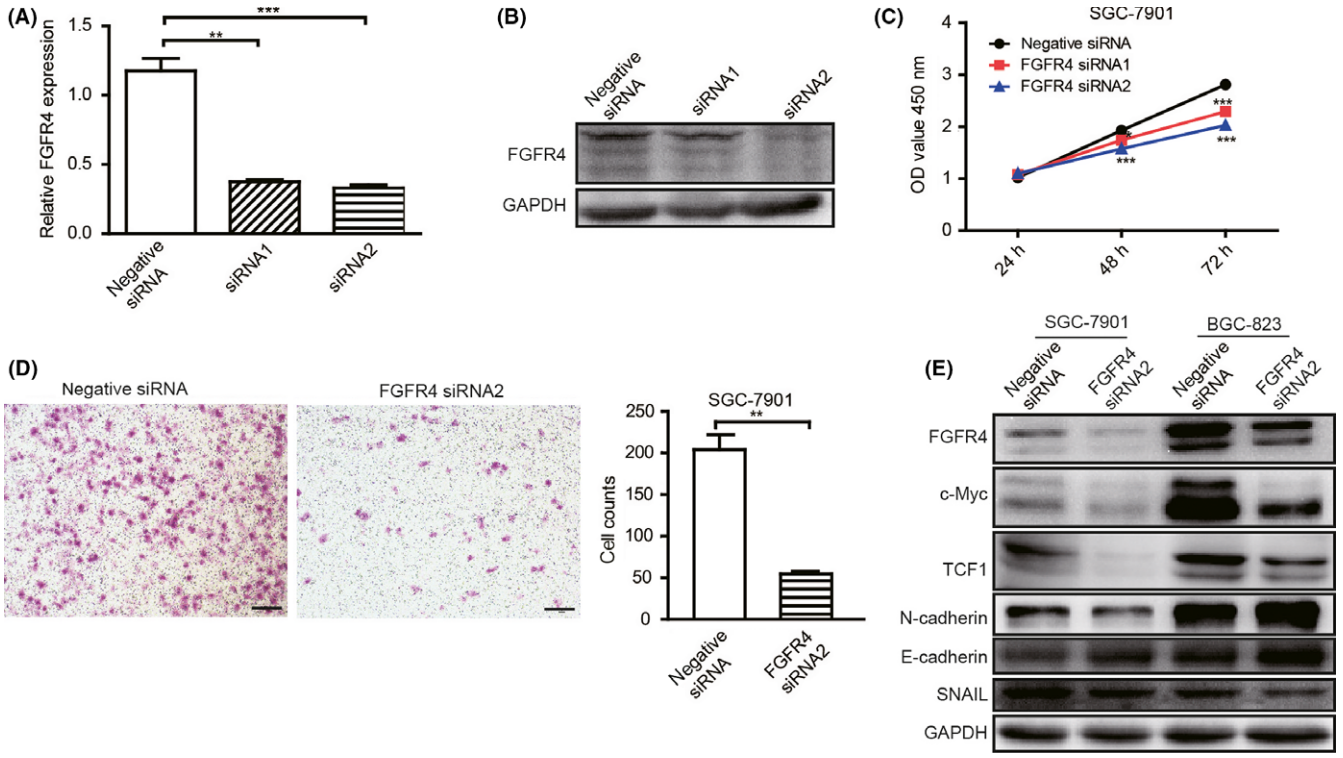

FIGURE 4 FGFR4 promotes gastric cancer (GC) cell proliferation and migration. The mRNA (A) and the protein (B) levels of FGFR4 in SGC-7901 cells transfected with siRNA. The proliferation (C) and the migration (D) abilities of SGC-7901 cells transfected with siRNA were detected at the indicated times. Scale bar = 50 μm. E, The protein levels of specific genes in SGC-7901 and BGC-823 cells transfected with FGFR4 siRNA. $^{**}P < .01$, $^{***}P < .001$

3.5 | Restoration of miR-491-5p decreases gastric cancer growth and metastasis in vivo

To explore the role of miR-491-5p in vivo, we constructed GC cell lines that stably overexpressed miR-491-5p (Figure S5). To remain close to a biological state, a low-titer infection was implemented to ensure an increase in miR-491-5p expression of approximately 3-fold (Figure 5A). Several characterized animal models, including a tumor xenograft model and abdominal dissemination and distal pulmonary metastasis models, were utilized. The results obtained from the tumor xenograft model revealed that the restoration of miR-491-5p in SGC-7901 cells inhibited xenograft growth in nude mice (Figure 5B,C). We examined the expression of SNAIL in the tumor nodules via IHC and found that the SNAIL level was decreased in the miR-491-5p-overexpressing group (Figure 5D). In the abdominal dissemination assays, miR-491-5p-overexpressing cells elicited abdominal tumor nodules that were obviously decreased compared with the nodules observed in the controls (Figure 5E). The protein levels of SNAIL, FGFR4, N-cadherin and c-Myc in the tumor nodules were reduced in the miR-491-overexpressing group (Figure 5F). In the distal pulmonary metastasis assays, miR-491-5p-overexpressing animals had fewer tumor nodules in the lungs (Figure 5G). These results suggest that miR-491-5p effectively inhibits GC growth and metastasis in vivo.

4 | DISCUSSION

Recently, a series of publications have demonstrated that miR-491-5p serves as an important tumor suppressor in cancer. miR-491-5p was first known for its significant role in promoting tumor cell apoptosis by targeting the anti-apoptotic factor Bcl-xl in several cancers.[3,15,18] In addition, miR-491-5p inhibits tumor cell migration and invasion by targeting GIT1 and TPX2 in squamous cell carcinomas and esophageal cancer, respectively.[4,19] In GC, the investigation of miR-491-5p is only beginning. Sun et al discovered that miR-491-5p inhibits GC growth by targeting Wnt3a. Here, we demonstrated that miR-491-5p expression was remarkably decreased in GC tissues and was associated with tumor size and different histological types. More importantly, we are the first to discover that miR-491-5p is a potent tumor suppressor of GC metastasis both in vitro and in vivo. We demonstrated that the restoration of miR-491-5p significantly inhibited GC peritoneal dissemination and pulmonary metastasis. Mechanistically, miR-491-5p directly targeted SNAIL to block EMT, and miR-491-5p suppressed the level of FGFR4, which led to further inhibition of SNAIL. Through the above mechanisms, downregulation of miR-491-5p induced EMT and promoted tumor metastasis (Figure 6).

SNAIL is essential for triggering EMT and promoting cancer progression. SNAIL is upregulated in GC and is associated with tumor progression and a poor prognosis.[20-22] We and others have found

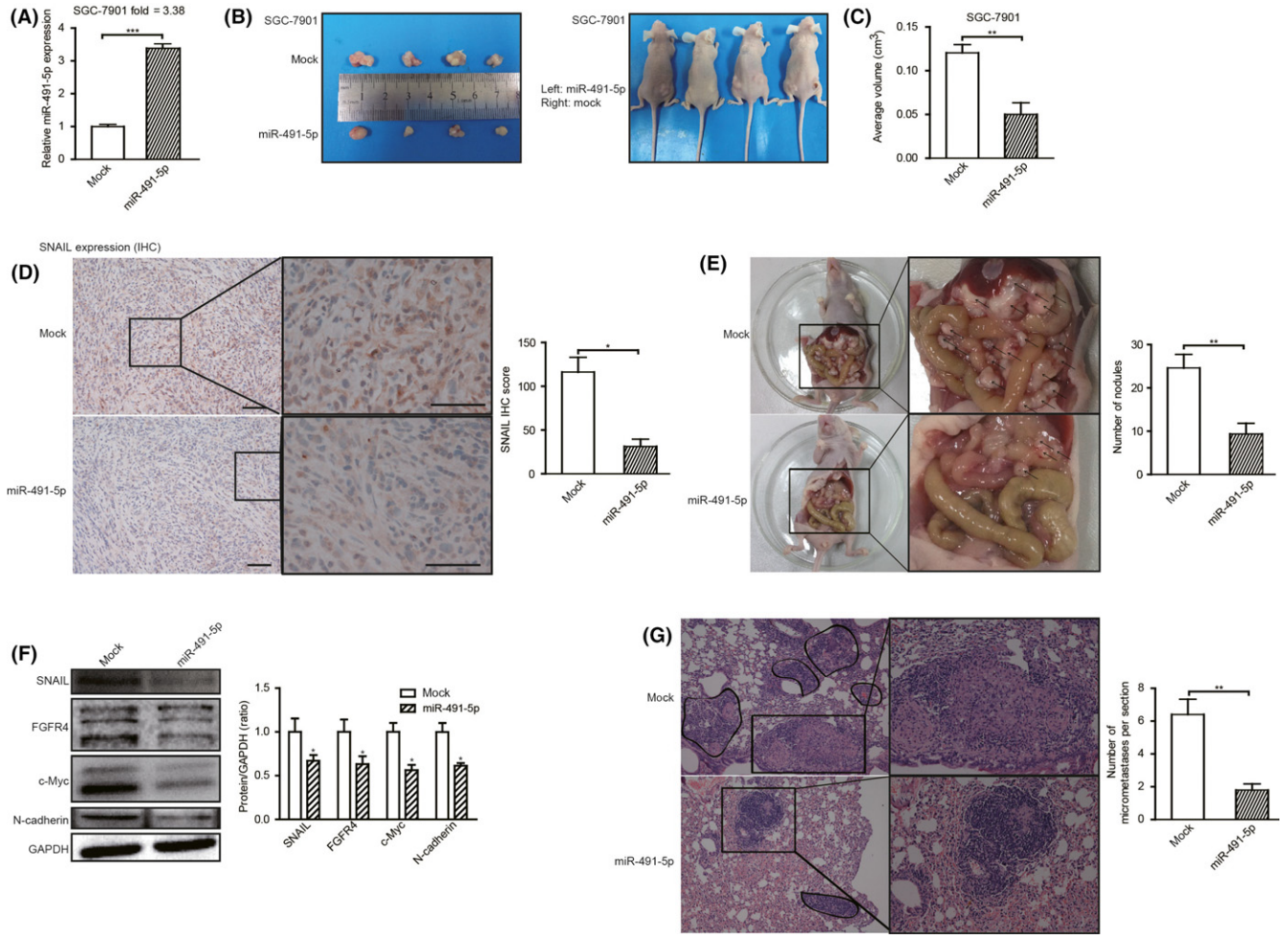

FIGURE 5 miR-491-5p inhibits gastric cancer (GC) metastasis in vivo. A, Relative expression of miR-491-5p in SGC-7901 cells infected with retrovirus. B, Tumor nodules from the tumor-bearing mice (left) and aspects of the tumor-bearing mice at day 30 (right). C, The statistics for the xenograft tumor volumes; n = 4 vs 4. D, SNAIL expression levels in the tumor nodules were assessed by immunohistochemistry at 200× magnification. Left: The representative images are presented. Right: Statistical analysis of the scores of SNAIL immunostaining; n = 4 vs 4. E, Tumor nodules in the abdominal cavities of the mice were examined. Right: Statistical analysis of the nodules number; n = 5 vs 5. F, The protein levels of SNAIL, FGFR4, c-Myc and N-cadherin in the tumor nodules in the abdominal cavities of the mice. Left: The representative protein bands are presented. Right: Quantitative analyses of the western blotting results; n = 5 vs 5. G, HE staining results of lung biopsies from the miR-491-5p-overexpressing group and the mock group. Right: Statistical analysis of the number of micrometastases per section; n = 5 vs 5. $^{**}P < .01$, $^{***}P < .001$

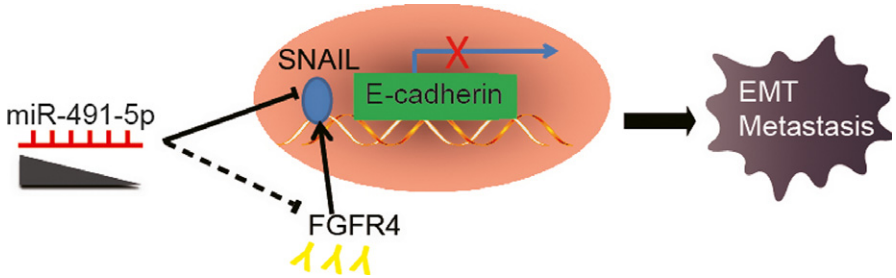

FIGURE 6 Schematic depicting how decreased miR-491-5p expression promotes epithelial-to-mesenchymal transition (EMT) in gastric cancer (GC) cells and results in GC metastasis. miR-491-5p, which is downregulated in GC, directly targets SNAIL to promote the transcription of E-cadherin; meanwhile, miR-491-5p indirectly inhibits FGFR4, which results in the suppression of SNAIL and the upregulation of E-cadherin. Finally, the downregulation of miR-491-5p leads to the inhibition of SNAIL, which induces EMT and promotes GC metastasis

that a series of miRNAs, including miR-22, miR-200c and miR-122, directly target SNAIL to suppress EMT and tumor progression.[8,23,24] Here, we identified SNAIL as a novel target of miR-491-5p. The level of SNAIL was inversely correlated with the level of miR-491-5p and associated with a poor prognosis. Gain-of-function and loss-of-function experiments indicated that SNAIL could partially mediate the tumor suppressive function of miR-491-5p.

FGFR4 is also an inducer of EMT and is capable of promoting cancer metastasis.[25,26] In GC, Ye et al[10] found that FGFR4 is highly expressed in GC tissues and correlates with lymph node status and prognosis, and promotes GC cell proliferation and decreases cell apoptosis. Here, we found that inhibition of FGFR4 led to a decreased level of SNAIL and suppressed EMT in GC. The level of FGFR4 correlated positively with the level of SNAIL and was associated with a poor prognosis. Although FGFR4 was predicted to be targeted by miR-491-5p based on TargetScan, the dual luciferase assay results revealed that miR-491-5p did not bind directly to the 3′-UTR of *FGFR4*. This discrepancy may be attributable to a false-positive prediction from the software, the complexity of miRNA-mRNA interactions in cells or the incomplete modeling of the physiological state by the experimental conditions. Given that FGFR4 was not a direct target of miR-491-5p, we speculate that miR-491-5p could regulate SNAIL indirectly in an FGFR4-dependent manner. However, the details of the regulatory effect of miR-491-5p on FGFR4 require further investigation.

Currently, the upstream regulatory mechanisms of miR-491-5p are not fully understood. miR-491-5p is reportedly induced by Foxi1 in GC cells and by TGF-β in rat proximal tubular epithelial cells and $CD8^+$ T cells.[6,11,27] However, in this study, TGF-β was not able to induce miR-491-5p after 3 days of observation in either SGC-7901 or BGC-823 cells (data not shown). These discrepancies may be due to the use of different cell types. We speculate that other factors, such as transcription factors or competing endogenous RNA, may participate in the regulation of miR-491-5p expression, and this speculation requires further investigation.

The transcript of miR-491 produces 2 mature products (i.e. miR-491-5p and miR-491-3p). Li et al[3] found that both miR-491-5p and miR-491-3p suppress glioblastoma proliferation, invasion and stem cell propagation. In this study, we found that miR-491-3p was downregulated in GC and was capable of inhibiting GC cell migration. These results suggest that miR-491-5p and miR-491-3p may coordinate to play key roles in GC and even in other types of cancer.

In conclusion, because miR-491-5p has been linked to growth inhibition and apoptosis promotion in GC, we provided new evidence that miR-491-5p inhibits GC metastasis both in vitro and in vivo. Mechanistically, miR-491-5p regulated the E-cadherin/N-cadherin balance by regulating SNAIL both directly and indirectly, which resulted in the repression of EMT and GC metastasis. Through this study, we hope to provide novel and comprehensive insights into the functional role of miR-491-5p in GC and to encourage the consideration of miR-491-5p as a putative treatment target for GC.

CONFLICT OF INTEREST

The authors have no conflict of interest to declare.

ORCID

Bin Xiao http://orcid.org/0000-0002-7087-8586

REFERENCES

1. Chen W, Zheng R, Baade PD, et al. Cancer statistics in China, 2015. *CA Cancer J Clin*. 2016;66:115-132.
2. Ueda T, Volinia S, Okumura H, et al. Relation between microRNA expression and progression and prognosis of gastric cancer: a microRNA expression analysis. *The Lancet Oncology*. 2010;11:136-146.
3. Li X, Liu Y, Granberg KJ, et al. Two mature products of MIR-491 coordinate to suppress key cancer hallmarks in glioblastoma. *Oncogene*. 2015;34:1619-1628.
4. Huang WC, Chan SH, Jang TH, et al. miRNA-491-5p and GIT1 serve as modulators and biomarkers for oral squamous cell carcinoma invasion and metastasis. *Cancer Res*. 2014;74:751-764.
5. Wang SN, Luo S, Liu C, et al. miR-491 Inhibits osteosarcoma lung metastasis and chemoresistance by targeting alphaB-crystallin. *Mol Ther*. 2017;25:2140-2149.
6. Sun R, Liu Z, Tong D, et al. miR-491-5p, mediated by Foxi1, functions as a tumor suppressor by targeting Wnt3a/beta-catenin signaling in the development of gastric cancer. *Cell Death Dis*. 2017;8:e2714.
7. Ushijima T. Sasako M Focus on gastric cancer. *Cancer Cell*. 2004;5:121-125.
8. Zuo QF, Cao LY, Yu T, et al. MicroRNA-22 inhibits tumor growth and metastasis in gastric cancer by directly targeting MMP14 and Snail. *Cell Death Dis*. 2015;6:e2000.
9. Pai R, Dunlap D, Qing J, et al. Inhibition of fibroblast growth factor 19 reduces tumor growth by modulating beta-catenin signaling. *Cancer Res*. 2008;68:5086-5095.
10. Ye YW, Zhou Y, Yuan L, et al. Fibroblast growth factor receptor 4 regulates proliferation and antiapoptosis during gastric cancer progression. *Cancer*. 2011;117:5304-5313.
11. Yu T, Zuo QF, Gong L, et al. MicroRNA-491 regulates the proliferation and apoptosis of CD8(+) T cells. *Sci Rep*. 2016;6:30923.
12. Li BS, Zuo QF, Zhao YL, et al. MicroRNA-25 promotes gastric cancer migration, invasion and proliferation by directly targeting transducer of ERBB2, 1 and correlates with poor survival. *Oncogene*. 2015;34:2556-2565.
13. Wang TT, Zhao YL, Peng LS, et al. Tumour-activated neutrophils in gastric cancer foster immune suppression and disease progression through GM-CSF-PD-L1 pathway. *Gut*. 2017;66:1900-1911.
14. Wroblewski LE, Piazuelo MB, Chaturvedi R, et al. Helicobacter pylori targets cancer-associated apical-junctional constituents in gastroids and gastric epithelial cells. *Gut*. 2015;64:720-730.
15. Denoyelle C, Lambert B, Meryet-Figuiere M, et al. miR-491-5p-induced apoptosis in ovarian carcinoma depends on the direct inhibition of both BCL-XL and EGFR leading to BIM activation. *Cell Death Dis*. 2014;5:e1445.
16. Zheng GP, Jia XT, Peng C, et al. The miR-491-3p/mTORC2/FOXO1 regulatory loop modulates chemo-sensitivity in human tongue cancer. *Oncotarget*. 2015;6:6931-6943.
17. Szasz AM, Lanczky A, Nagy A, et al. Cross-validation of survival associated biomarkers in gastric cancer using transcriptomic data of 1,065 patients. *Oncotarget*. 2016;7:49322-49333.
18. Nakano H, Miyazawa T, Kinoshita K, et al. Functional screening identifies a microRNA, miR-491 that induces apoptosis by targeting Bcl-X(L) in colorectal cancer cells. *Int J Cancer*. 2010;127:1072-1080.

19. Niu H, Gong L, Tian X, et al. Low expression of miR-491 promotes esophageal cancer cell invasion by targeting TPX2. *Cell Physiol Biochem*. 2015;36:2263-2273.
20. Shin NR, Jeong EH, Choi CI, et al. Overexpression of Snail is associated with lymph node metastasis and poor prognosis in patients with gastric cancer. *BMC Cancer*. 2012;12:521.
21. Zou S, Ma C, Yang F, et al. FBXO31 Suppresses gastric cancer EMT by targeting Snail1 for proteasomal degradation. *Mol Cancer Res*. 2017;16:286-295.
22. Wu W, Ding H, Cao J, et al. FBXL5 inhibits metastasis of gastric cancer through suppressing Snail1. *Cell Physiol Biochem*. 2015;35:1764-1772.
23. Perdigao-Henriques R, Petrocca F, Altschuler G, et al. miR-200 promotes the mesenchymal to epithelial transition by suppressing multiple members of the Zeb2 and Snail1 transcriptional repressor complexes. *Oncogene*. 2016;35:158-172.
24. Jin Y, Wang J, Han J, et al. MiR-122 inhibits epithelial-mesenchymal transition in hepatocellular carcinoma by targeting Snail1 and Snail2 and suppressing WNT/beta-cadherin signaling pathway. *Exp Cell Res*. 2017;360:210-217.
25. Liu R, Li J, Xie K, et al. FGFR4 promotes stroma-induced epithelial-to-mesenchymal transition in colorectal cancer. *Cancer Res*. 2013;73:5926-5935.
26. Zhao H, Lv F, Liang G, et al. FGF19 promotes epithelial-mesenchymal transition in hepatocellular carcinoma cells by modulating the GSK3beta/beta- catenin signaling cascade via FGFR4 activation. *Oncotarget*. 2016;7:13575-13586.
27. Zhou Q, Fan J, Ding X, et al. TGF-{beta}-induced MiR-491-5p expression promotes Par-3 degradation in rat proximal tubular epithelial cells. *J Biol Chem*. 2010;285:40019-40027.

SUPPORTING INFORMATION

Additional Supporting Information may be found online in the supporting information tab for this article.

How to cite this article: Yu T, Wang L-N, Li W, et al. Downregulation of miR-491-5p promotes gastric cancer metastasis by regulating SNAIL and FGFR4. *Cancer Sci*. 2018;109:1393-1403. https://doi.org/10.1111/cas.13583